Vol 18 No 9, September 2009
1674-1056/2009/18(09)/3985-05

Chinese Physics B

© 2009 Chin. Phys. Soc.
and IOP Publishing Ltd

Highly sensitive room-temperature gas sensors based on hydrothermal synthesis of Cr_2O_3 hollow nanospheres*

Li Sheng(李 盛), Li Feng-Li(李凤丽), Zhou Shao-Min(周少敏)†,
Wang Peng(王 鹏), Cheng Ke(程 轲), and Du Zu-Liang(杜祖亮)

Key Lab for Special Functional Materials of Ministry of Education, Henan University, Kaifeng 475004, *China*

(Received 30 November 2008; revised manuscript received 28 February 2009)

This paper reports that Cr_2O_3 hollow nanospheres (HNs) were synthesized via a hydrothermal approach and characterized by scanning electron microscopy, x-ray powder diffraction, transmission electron microscopy (TEM), selective area electron diffraction and high resolution TEM, respectively. In addition, the room-temperature (RT) gas sensing properties of Cr_2O_3 HNs and conventional powders (CPs) were investigated by means of the surface photovoltage technique. The experimental data demonstrate that the RT gas sensor of the as-fabricated HNs reaches below 5 ppm whereas that of the CPs is about 40 ppm, which results from there being much more adsorbed and desorbed oxygen in HNs than in CPs at RT. The as-prepared Cr_2O_3 HNs could have potential applications as RT nanosensors.

Keywords: Cr_2O_3, hollow nanospheres, gas sensing, surface photovoltage
PACC: 7300, 7240, 8116, 7125R

1. Introduction

As an important wide band gap semiconductor, Cr_2O_3 has many outstanding properties, such as catalysis,[1] electrochemical,[2] magnetic,[3,4] optoelectronic,[5] mechanical[6] and gas sensing[7]*properties*. Recently, many researchers have reported on the gas sensing properties of doped and un-doped Cr_2O_3 films at high temperatures. For example, the gas sensing properties of Fe_2O_3-activated Cr_2O_3 thick films are dependent on temperature from 500 K to 800 K.[8] Reference [9] reported that, above an alcohol concentration of 20 ppm, the resistance of Cr_2O_3 thin film began to change obviously at 600 K. However, there was still a fatal problem. It is difficult for these film gas sensors to operate in practice, because they cannot work at room temperature (RT) and low concentrations of target gases.[10−14]

Several reports devoted to semiconductor gas sensors have shown the importance of enhancing the oxide surface area[15−17] since Kawi and co-workers demonstrated that an increase in this parameter improved the sensor response.[18] Within this context, it has become an important issue for the synthesis of semiconductor oxides with mesoporous structure presenting uniform small sizes of stabilized crystals and large active surface areas. Hollow nanospheres (HNs), as typical three-dimensional curved structures with inner cavities, are of much importance because of their unique properties of low density, high specific surface area, good permeation and their potential applications in various areas.[19,20] So far, hollow spheres of many materials have been fabricated through various methods, including template assisted synthesis,[21] direct evacuations with Ostwald ripening and the Kirkendall effect.[22] Here, we have synthesized Cr_2O_3 HNs using carbonaceous polysaccharide microspheres as templates by a simple hydrothermal route.

As far as we know, most of the traditional resistance types of sensors should run at high temperature (about $> 300\ ^\circ$C) and high gas concentration, because gas adsorption-desorption is carried out very slowly at RT.[23,24] On the other hand, the surface photovoltage (SPV) method is a well established contactless and nondestructive technique for semiconductor characterization that relies on analysing illumination-induced changes in the surface voltage.[25,26] In recent years, the SPV technique has been increasingly

*Project sponsored by the Program for Science & Technology Innovation Talents in Universities of Henan Province (Grant No 2008 HASTIT002), the Innovation Scientists and Technicians Troop Construction Projects of Henan Province of China and the National Natural Science Foundation of China (Grant No 20941002).
†E-mail: smzhou@henu.edu.cn

used to investigate the gas sensing properties mainly due to the rapid and highly sensitive detection of gas sensing materials at RT.[27,28] In this paper, we also study the gas sensing properties of Cr_2O_3 HNs by the SPV technique and explain the experimental results through the theory of energy bands. To the best of our knowledge, this is the first report on the gas sensing of Cr_2O_3 HNs by the SPV method.

2. Experimental

$Cr(NO_3)_3{\cdot}9H_2O$ (99.9%), Cr_2O_3 CPs (99.99%) and glucose (99.8%) were used without further purification. In a standard experiment, glucose (0.8 mmol) and $Cr(NO_3)_3{\cdot}9H_2O$ (0.1 mmol) were dissolved in 20 ml distilled water and 10 ml distilled water, respectively. Here the carbohydrate : chromium (molar ratio) was 8:1 though varying carbohydrate : chromium (molar ratios) can be used, from 15:1 to 2:1. Then the two solutions were mixed immediately and placed in a 45 ml capacity Teflon-lined stainless steel autoclave, which was heated in an oven from RT to 180 °C for 24 h. The mid-products were filtered off and washed several times: first with distilled water, then with ethanol, and were finally dried in a vacuum oven at 60 °C for 5 h. After that, the metal oxide-carbon composites were calcined in air at 550 °C (heating rate of 1 °C/min) for 4 h to remove the carbon core; this leads to Cr_2O_3 HNs.

The products were characterized extensively for morphology, phase, growth direction and chemical composition by using scanning electron microscopy (SEM, JEOL JSM-5600LV, Japan), x-ray powder diffraction (XRD, X'Pert Pro), transmission electron microscopy (TEM, JEM 100CX-II), selective area electron diffraction (SAED) and high resolution TEM (HRTEM, JEM-2010).

The SPV instrument was homemade. Monochromatic light was obtained by passing light from a 500 W xenon lamp (CHF XQ500W, Global xenon lamp power made in China) through a double-prism monochromator (Zolix Omni-λ 500, made in China). The slit widths of the entrance and exit are 1 mm. A lock-in amplifier (SR830-DSP, made in the USA) synchronized with a light chopper (SR540, made in the USA) was employed to amplify the photovoltage signal. The range of modulating frequency is from 20 to 70 Hz and the spectral resolution is 1 nm. The raw SPV data were normalized by using an illuminometer (Zolix UOM-1S, made in China). The samples were studied without further treatment during the SPV measurements, in which the contact between samples and indium tin oxide (ITO) electrodes is not an ohmic contact since we carried out the measurement of SPV.

3. Results and discussion

Figure 1(a) displays a panoramic SEM image of the Cr_2O_3 HNs, which shows that the obtained sample consists of large-scale hollow spheres with diameters about 0.3–4 μm. The hollow nature of the nanospheres could be clearly concluded from the broken spheres as shown in a typical high magnification SEM (HMSEM) image (the left inset of Fig.1(a)). Based on the HMSEM, the thickness of the broken spheres is about 50 nm. As shown in Fig.1(b), in the diffraction patterns of the Cr_2O_3 HNs we have not found any other impurity peaks in comparison with the standard values of Cr_2O_3 bulk crystal structure (Card No.85-0869, JCPDS-ICDD). In addition, statistics on the HNs' size found as a function of the NHs' numbers are presented in Fig.1(c). The HN size distribution is not very uniform, which may result from the uneven size of the carbon spheres. Almost half the numbers of the NHs' size are about 0.5–1 μm.

A representative TEM image of the Cr_2O_3 HNs sample is shown in Fig.2(a), in which sphere-like products with diameters of 300–600 nm can be seen and are compatible with the SEM results. Figure 2(b) is an emblematical SAED pattern from the products and polycrystalline structures were found. A HRTEM image of the Cr_2O_3 HNs is indicated in Fig.2(c). The marked interplanar *d*-spacings of about 0.144 nm correspond to the lattice constant of Cr_2O_3, which is in agreement with these results of XRD and SAED.

As for the HNs' growth, we assume that the formation of the carbon spheres firstly involves the dehydration of the carbohydrate and carbonization of the so-formed organic compounds, whose surface is hydrophilic and has a distribution of OH and C=O groups. Then, during the reaction, Cr^{3+} and its resulting nanoparticles are predominantly positioned near the hydrophilic shell of the carbon particles, which yields an increase in the diameter of the carbon spheres. After annealing, the carbon spheres are removed, Cr^{3+} is oxidated and Cr_2O_3 HNs are obtained as shown in Fig.2(d).

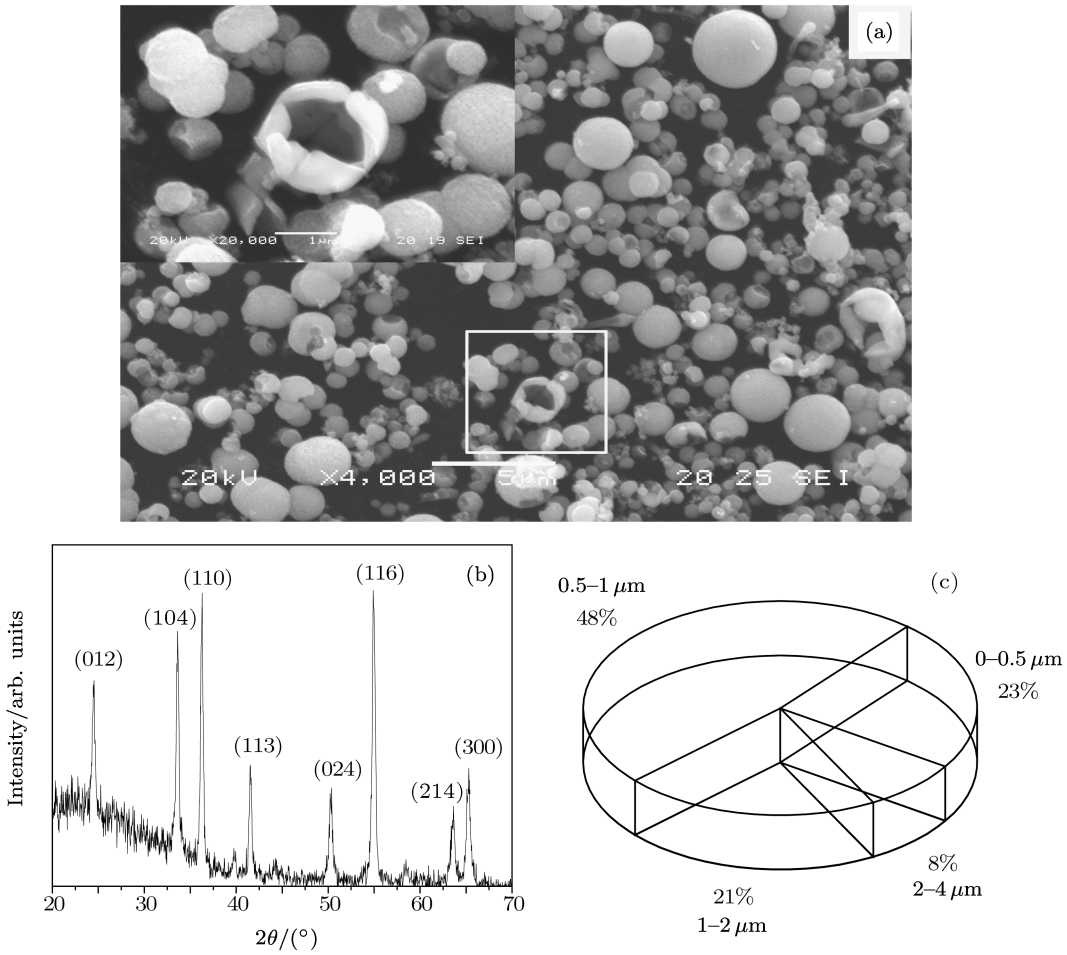


Fig.1. (a) A low-magnification SEM image and HMSEM image (left inset); (b) XRD patterns of the collected product; (c) statistics of the HNs' size for NHs with diameters between 0 and 4 μm.

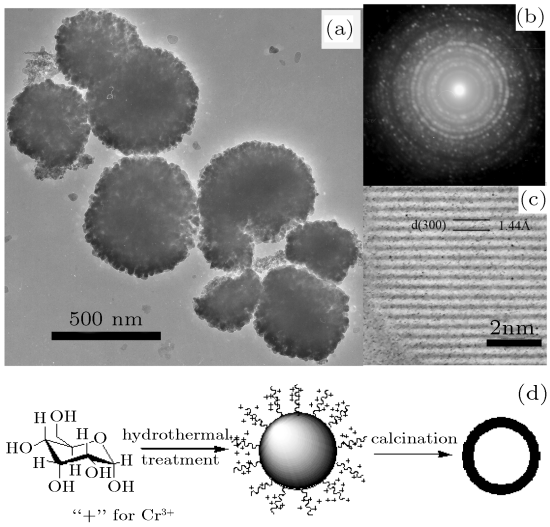


Fig.2. (a) A typical TEM image of Cr_2O_3 HNs; (b) A typical SAED pattern; (c) An HRTEM image of the HNs exhibiting marked interplanar d-spacings ($\sim$ 1.44 Å) corresponding to the {300} lattice fringes of the Cr_2O_3 HNs; (d) Proposed growth model for Cr_2O_3 HNs.

The gas sensing properties were measured by SPV technology. The construction of the photovoltaic cell is a sandwich structure (see the inset of Fig.3(a)). Typical RT SPV spectra of the Cr_2O_3 HNs and conventional powers (CPs) in air and ethanol (5 ppm) are respectively shown in Fig.3(a). It can be observed that the SPV responses of the two samples are similar in air whereas there is a huge change in ethanol. For example, the SPV of HNs reaches about 7.8 mV at 370 nm in ethanol whereas that of CPs is $\sim$ 3.6 mV at the same condition. In order to illustrate the relationship between the sensing and the gas concentration clearly, we defined the gas sensitivity as $\mathrm{Sen} = (V_\mathrm{b} - V_\mathrm{a})/V_\mathrm{a}$, where V_a and V_b are the SPV of the sensor in air and ethanol, respectively. Figure 3(b) is used to indicate the plots of sensitivity versus the vapour concentration when HNs and CPs were exposed to ethanol. Obviously, the sensitivities of the two samples increase with an increase of ethanol concentration; nevertheless, the Cr_2O_3 HNs are more sensitive than Cr_2O_3 CPs.

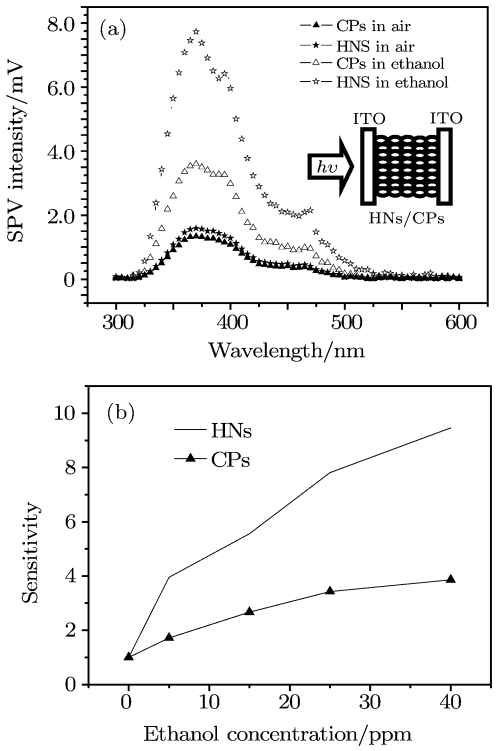


Fig.3. (a) SPV spectra of two samples (HNs and CPs) in air and ethanol respectively. Inset: scheme of the SPV experimental cell and the sample condition; (b) sensitivity of the Cr_2O_3 HNs and Cr_2O_3 CPs in ethanol.

Since Cr_2O_3 is a typical p-type semiconductor and its Fermi level is below the Fermi level of the surface states,[29,30] part of the electronics will transfer from a high-energy position (surface states) to a low-energy position (Fermi level). As a result, the surface is positively charged whereas the bulk phase is negative, i.e. a built-in electric field is formed. Also, the energy bands will lead to a downward bending in the space charge region. In this case, under the effect of the built-in electric field, the photogenerated electron–hole pairs are separated and the corresponding SPV responses produced.[31]

To explain the gas sensing properties, the chemical potentials of Cr_2O_3, O_2, O_2^- and C_2H_5OH are given in Table 1. As we know, the Fermi level is equivalent to the chemical potential in the system. In this way, according to the different Fermi levels (see Table 1), we describe the schematic diagram of Cr_2O_3 HNs' band bending through the entire experimental process (shown in Fig.4).

Table 1. The chemical potential of Cr_2O_3, O_2, O_2^- and C_2H_5OH.

	Cr_2O_3	O_2	O_2^-	C_2H_5OH
chemical potential/(kJ/mol)	–1058.13	0	–42.57	–168.57

For illumination, the photogenerated electrons transferred to the surface whereas the holes moved to the bulk by the built-in electric field E_b, whose direction is from the surface to the bulk.[32,33] At the same time, the adsorbed oxygen on the surface would combine with the electrons and generate the ionosorbed oxygen. As electrons transferred from the bulk to the surface, weakening the self-built electric field and depletion layer, the band bending should reduce. At the equilibrium state, ΔE_a (the variable of the energy band bending in air) is obtained, which is equivalent to the V_a in experiment. When ethanol is exposed, the alcohol molecule may restore the ionosorbed oxygen and release free electrons. Therefore, the amount of the electrons on the surface will increase in the ethanol system (the corresponding SPV responses changed more strongly). In contrast, the energy band bending would continue to weaken.

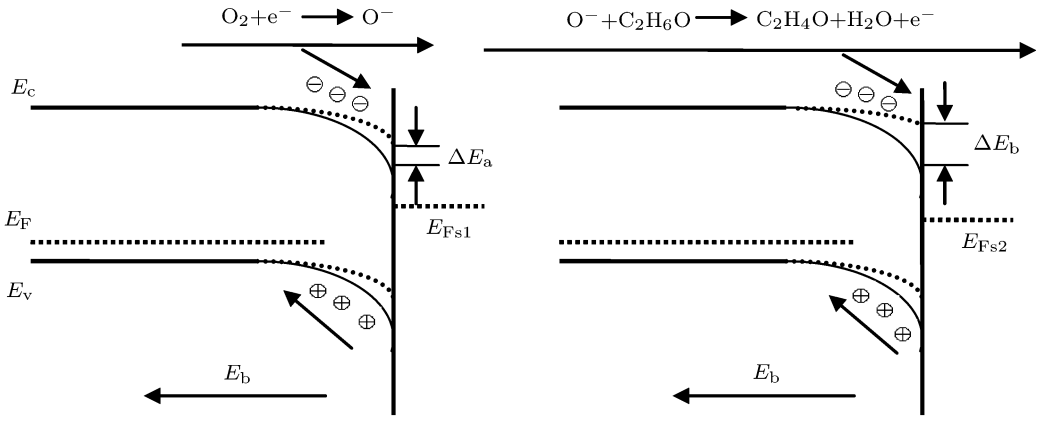


Fig.4. Schematic diagram of Cr_2O_3 HNs' energy band bending. E_c, E_v and E_F are the conduction band, valence band and Fermi level, respectively. E_b is the built-in electric field. E_{Fs1} and E_{Fs2} are the Fermi levels of the surface states in air and in ethanol respectively. Based on the chemical potential, $E_{Fs1} > E_{Fs2}$.

In a similar manner, ΔE_b (the variable of the energy band bending in ethanol) could be obtained. Since ΔE_b is larger than ΔE_a, we can successfully explain the different SPV in air and ethanol based on the changes in energy band bending.

But why are both samples (the CPs and the NHs) similar in air but very different in ethanol? The reason may be that the porous architecture of the HNs provides more sufficient space and active sites enabling both the target species and the background gas to access all the surface of Cr_2O_3 HNs contained in the sensing unit, thus improving the efficiency of gas diffusion and the interaction between adsorbed oxygen ions and detected gases. The high sensitivity under ambient conditions can be attributed to the intrinsic mesoporosity and high surface-to-volume ratio associated with the mesoporous hollow spheres.[34,35] Of course, the corresponding mechanism still requires more systematic and extensive study.

4. Conclusions

In summary, we have synthesized Cr_2O_3 HNs in solution phase by using novel carbon microspheres as templates. With the nanoporous structure, it was found that Cr_2O_3 HNs have good sensitivity in low concentrations of alcohol at RT by SPV technology. We believe that Cr_2O_3 HN gas sensors might have promising applications in the future and stimulate research for other kinds of nanostructure gas sensors.

References

[1] Yamashita H, Ohshiro S, Kida K, Yoshizawa K and Anpo M 2003 *Res. Chem. Intemed.* **29** 881

[2] Hu J, Li H, Huang X J and Chen L Q 2006 *Solid. State. Ionics.* **177** 2791

[3] Pop I, Andrecut M, Burda I, Oprea C, Andrecut C and Mater J 1997 *Sci. Lett.* **16** 2052

[4] Krotov S S, Popov Y F, Kadomtseva A M, Belov D V, Vorob'ev G P and Lisniak A V 2002 *Ferroelectrics.* **280** 145

[5] Ivanova T, Gesheva K A, Sharlandjiev P and Georgieva A K 2007 *Surf. Coat. Technol.* **201** 9313

[6] Cetinel H, Celik E and Kusoglu M I 2008 *J. Mater. Process. Technol.* **196** 259

[7] Yoo J H and Wachsman E D 2006 *ECS. Trans.* **1** 173

[8] Suryawanshi D N, Patil D R and Patil L A 2008 *Sens. Actuators* B **134** 579

[9] Pokhrel S, Simion C E, Quemener V, Barsan N and Weimar U 2008 *Sens. Actuators* B **133** 78

[10] Buzzeo M, Hardacre C and Compton R 2004 *Anal. Chem.* **76** 4583

[11] Boarino L, Baratto C, Geobaldo F, Amato G, Comini E, Rossi A M, Faglia G, Lerondel G and Sberveglieri G 2000 *Mater. Sci. Eng.* B **69** 210

[12] Kim Y S, Ha S C, Kim K, Yang H, Choi S Y, Kim Y T, Park J T, Lee C H, Choi J, Paek J and Lee K 2005 *Appl. Phys. Lett.* **86** 213105

[13] Sun Z P, Liu L, Zhang L and Jia D Z 2006 *Nanotechnology* **17** 2266

[14] Geng B Y, Zhan F M, Fang C H and Yu N 2008 *J. Mater. Chem.* **18** 4977

[15] Zhang J T, Liu J F, Peng Q, Wang X and Li Y D 2006 *Chem. Mater.* **18** 867

[16] Zhang H, Wu J B, Zhai C X, Du N, Ma X Y and Yang D R 2007 *Nanotechnology* **18** 455604

[17] Tan O K, Cao W, Hu Y and Zhu W 2004 *Ceram. Int.* **30** 1127

[18] Li G J, Zhang X H and Kawi S 1999 *Sens. Actuators* B **60** 64

[19] Fowler C E, Khushalani D D and Mann S 2001 *Chem. Commun.* **19** 2028

[20] Huang H Y, Remsen E E, Kowalewski T and Wooley K L 1999 *J. Am. Chem. Soc.* **121** 3805

[21] Zhu Y Z, Yin J Q and Qiu M H 2008 *Acta Phys. Sin.* **57** 7725 (in Chinese)

[22] Yang H G and Zeng H C 2004 *J. Phys. Chem.* B **108** 3492

[23] Tan O K, Cao W, Zhu W, Chai J W and Pan J S 2003 *Sens. Actuators* B **93** 396

[24] Vaishnav V S, Patel P D and Patel N G 2005 *Thin Solid Films* **487** 277

[25] Zhu W Z and Shen K H 1996 *Acta Phys. Sin.* **45** 258 (in Chinese)

[26] Yu W, Wang C S, Lu W B, He J, Han X X and Fu G S 2007 *Chin. Phys.* **16** 8

[27] Li K Y, Wang D J, Wu F Q, Xie T F and Li T J 2000 *Mater. Chem. Phys.* **64** 269

[28] Li K Y, Wu F Q, Wang D J, Xie T F and Li T J 2001 *Mater. Chem. Phys.* **71** 34

[29] Kronik L and Shapira Y 2001 *Surf. Interface. Anal.* **31** 954

[30] Cao H Q, Qiu X Q, Liang Y, Zhao M J and Zhu Q M 2006 *Appl. Phys. Lett.* **88** 241112

[31] Lin Y H, Wang D J, Zhao Q D, Li Z H, Ma Y D and Yang M 2006 *Nanotechnology* **17** 2110

[32] Zhao S Q, Zhou Y L, Zhao K, Wang S F, Chen Z H, Lü H B, Jin K J, Cheng B L and Yang G Z 2006 *Chin. Phys.* **15** 839

[33] Zhao K, Feng J F, Huang Y H, Zhao J G, Lü H B, Han X F and Zhan W S 2005 *Chin. Phys.* **14** 2595

[34] Wang Y L, Jiang X C and Xia Y N 2003 *J. Am. Chem. Soc.* **125** 16176

[35] Favier F, Walter E C, Zach M P, Benter T and Penner R M 2001 *Science* **293** 2227